

An anomaly in the temperature dependence of the resistivity of amorphous metallic $\text{Fe}_x\text{Ge}_{1-x}$ alloys at low temperatures

This article has been downloaded from IOPscience. Please scroll down to see the full text article.

1995 J. Phys.: Condens. Matter 7 4649

(<http://iopscience.iop.org/0953-8984/7/24/006>)

View [the table of contents for this issue](#), or go to the [journal homepage](#) for more

Download details:

IP Address: 171.66.16.151

The article was downloaded on 12/05/2010 at 21:28

Please note that [terms and conditions apply](#).

An anomaly in the temperature dependence of the resistivity of amorphous metallic $\text{Fe}_x\text{Ge}_{1-x}$ alloys at low temperatures

A Albers and D S McLachlan

Department of Physics and Condensed Matter Physics Research Unit, University of the Witwatersrand, Private Bag 3, Wits 2050, South Africa

Received 1 September 1994, in final form 13 February 1995

Abstract. The anomalous decrease in the resistivity observed in the amorphous $\text{Cr}_x\text{Si}_{1-x}$, $\text{Cr}_x\text{Ge}_{1-x}$, and $\text{Fe}_x\text{Ge}_{1-x}$ systems as T decreases below about 30 K, and the subsequent increase in the resistivity as the temperature decreases below about 4 K are investigated in amorphous $\text{Fe}_x\text{Ge}_{1-x}$ films of nominal thickness 500 Å and 2000 Å for $0.189 \leq x \leq 0.297$. In this first detailed study the results of both resistivity and magnetoresistance measurements ($0.1 \leq T \leq 6$ K and $0 \leq B \leq 4$ T; $5 \leq T \leq 100$ K and $0 \leq B \leq 8.5$ T) are reported, and interpreted in terms of electron–electron interactions, weak localization, and spin fluctuations.

1. Introduction

Resistivity measurements on the amorphous $\text{Cr}_x\text{Si}_{1-x}$ (Möbius *et al* 1985), $\text{Cr}_x\text{Ge}_{1-x}$ (Elefant *et al* 1991), and $\text{Fe}_x\text{Ge}_{1-x}$ (Albers and McLachlan 1993) systems have shown the presence of a local maximum in the resistivity at about 30 K, with an anomalous decrease in ρ as the temperature is reduced below that temperature, reaching a local minimum at about 4 K, followed by an increase in ρ as the temperature is decreased further. It must be emphasized that this anomaly has never been observed in amorphous alloys of Ge or Si with non-magnetic elements. Furthermore, no detailed investigation of the resistivity and magnetoresistance concentrating specifically on the temperature regime between where the maximum and minimum in ρ occur has thus far been reported. To date only magnetoresistance measurements on the amorphous $\text{Fe}_x\text{Ge}_{1-x}$ system in the temperature range below the minimum in ρ have been presented in Albers and McLachlan (1993). It is therefore of interest to perform a thorough investigation of the resistivity and magnetoresistance behaviour in samples which exhibit this anomalous behaviour with the primary aim of ascertaining the characteristic temperature and magnetic field dependences, and then to attempt to identify the conduction mechanism(s) responsible by comparing the measured data with current relevant theories. Using the criteria from the theories of weak localization and impurity-enhanced electron–electron interactions, the 500 Å samples are expected to be three dimensional, but to confirm this expectation samples of 2000 Å thickness are also measured.

Based on the earlier less detailed results, the decrease in ρ as the temperature decreases below about 30 K has previously been tentatively interpreted as due to electron–electron interactions with enhanced screening of the Coulomb interactions (Elefant *et al* 1991, Mott and Davis 1991, Albers and McLachlan 1993), which would result in an unusual contribution

to the resistivity ρ proportional to \sqrt{T} . The increase in ρ as the temperature decreases below about 4 K has tentatively been interpreted as due to weak localization with the dominant inelastic scattering of the electrons by magnons (Mott 1990, Mott and Davis 1991, Albers and McLachlan 1993).

2. Experimental method

Amorphous $\text{Fe}_x\text{Ge}_{1-x}$ films of nominal thickness 500 Å and 2000 Å have been prepared on flame-polished glass substrates held at 195 K using Ar ion beam sputtering. The thickness of the samples was determined using a quartz crystal thickness monitor, and confirmed using a Talystep stylus. The sample composition and homogeneity was determined by energy dispersive spectroscopy (EDS) on a scanning electron microscope, using bulk Fe, Ge, and $\text{Fe}_{0.3}\text{Ge}_{0.7}$ standards. The amorphous structure was confirmed using electron diffraction on a transmission electron microscope. Further details of these techniques used are given elsewhere (Albers and McLachlan 1993, Albers 1994).

Four-point resistivity and magnetoresistance measurements were performed in three sets of experimental apparatus. Initial measurements of the resistance of all the samples between 273 K and 4.5 K or in some cases 2.0 K were made using a quick-measurement probe which was cooled by slowly inserting it into a liquid ^4He storage Dewar. The temperatures below 4.5 K were achieved by pumping on a small amount of liquid ^4He which was drawn into the vacuum-isolated sample space through a flow impedance consisting of a narrow capillary tube partially blocked by close-fitting metal wire. These initial resistance measurements showed that the anomalous decrease in ρ occurred in samples with between about 17 at.% Fe and 27 at.% Fe. Therefore, five nominally 500 Å thick and five nominally 2000 Å thick samples, with compositions spread evenly between about 17 at.% Fe and 27 at.% Fe, were selected for further measurements. In a conventional Janis Research Co. ^4He cryostat the magnetoresistance of the ten selected samples was measured at fixed temperatures between 5 K and 100 K (± 0.2 K for $T \geq 30$ K, and ± 0.01 K for $5 \text{ K} \leq T \leq 30 \text{ K}$), in varying fields ($B \perp I$ and $B \perp$ plane of sample) up to 8.5 T. In this system the magnetoresistance was measured as a function of field at fixed temperatures. In both of the above two experiments, the measurements were made using a DC measurement system with a current density of 6 A cm^{-2} , and an accuracy of 1 in 10^5 using a 6 $\frac{1}{2}$ -digit DVM. Using a dilution refrigerator, the resistance and magnetoresistance at temperatures varying between 6 K and typically 100 mK (to $\pm 1\%$) was measured in fixed fields from 0 to 4 T ($B \perp I$ and $B \parallel$ plane of film) using a Linear Research LR-400 AC resistance bridge to an accuracy of 1 in 10^5 with a current density of 60 mA cm^{-2} . According to the relevant theories the two field orientations used are equivalent, and this was confirmed by measurements between 6 K and 1.2 K.

3. Experimental results

The numbering, thickness, composition, and some characteristic resistivities of the samples are given in table 1. The observed resistivity as a function of temperature between 80 K and 4.5 K for representative nominally 500 Å and nominally 2000 Å samples is shown in figure 1(a) and (b) respectively. The decrease in ρ as T decreases below about 30 K, and the subsequent increase in ρ as T decreases below about 5 K, which are typical of the behaviour observed in both the 500 Å and 2000 Å samples, are clearly evident on this scale. Limited regions of $\rho \propto \sqrt{T}$ dependence can be identified in the ρ of all the samples in two temperature regimes, one between the maximum and the minimum in ρ , and the other

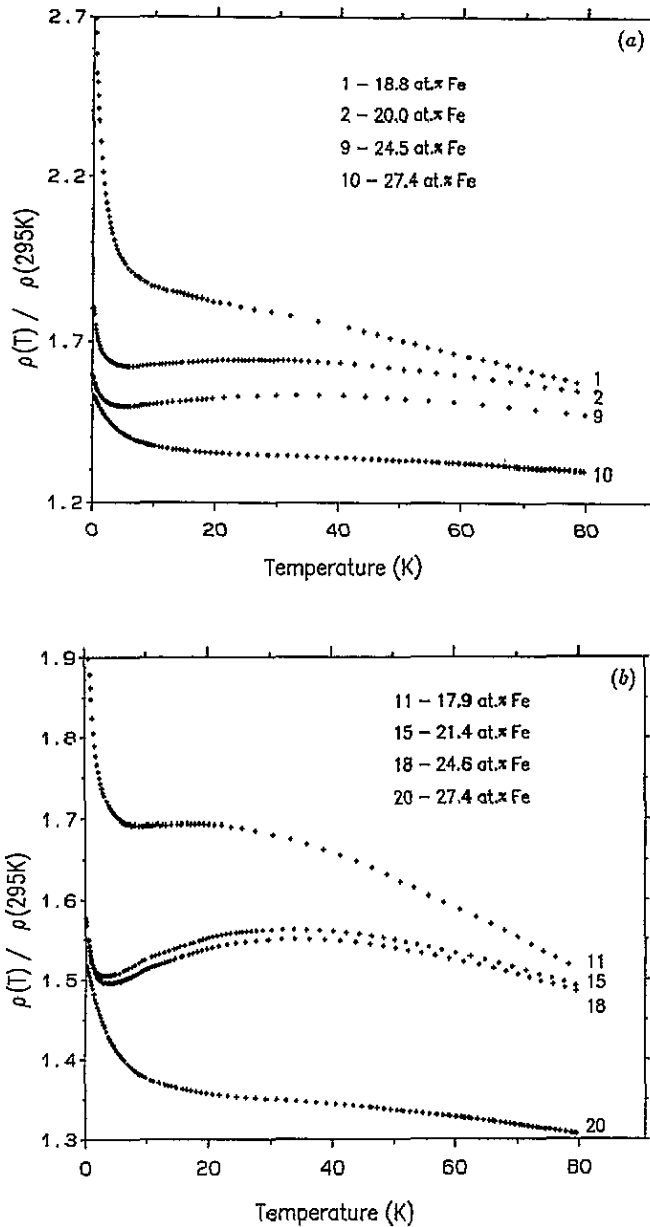


Figure 1. The measured $\rho(T)$ as a function of T below 80 K: (a) for four representative nominally 500 Å samples; (b) for four representative nominally 2000 Å samples. The data for each sample have been normalized to the value of $\rho(295\text{ K})$ given in table 1, and for samples 1, 11, and 20 displaced vertically by -0.15, -0.18, and +0.01 for clarity.

below the minimum in ρ (Albers and McLachlan 1993, Albers 1994). Above 80 K, the resistivity of all the samples shows the small negative temperature coefficient of resistance (TCR) behaviour which is typical of high-resistivity metallic samples (Mooij 1973).

The magnetoresistance at $1.5\text{ K} \leq T \leq 100\text{ K}$ in magnetic fields $B \leq 8.5\text{ T}$ of sample 2 (500 Å, 20.0 at.% Fe) is shown in figure 2(a). This figure illustrates the characteristic shape

Table 1. The thickness, composition, and characteristic resistivities of the samples.

| Name | Sample | Thickness (Å) | at.% Fe | $\rho(295\text{ K})$ ($\mu\Omega\text{ cm}$) | $\rho(5\text{ K})$ ($\mu\Omega\text{ cm}$) | $\Delta\rho/\rho(\text{min})$ (%) |
|-------|--------|---------------|---------|--|--|-----------------------------------|
| A2.58 | 1 | 510(10) | 18.8(3) | 2650(50) | 5500(100) | — |
| A2.33 | 2 | 530(10) | 20.0(3) | 2010(40) | 3260(60) | 1.291(1) |
| A2.38 | 3 | 530(10) | 20.5(3) | 1740(40) | 2710(50) | 1.827(1) |
| A2.40 | 4 | 530(10) | 20.9(3) | 1640(40) | 2560(50) | 2.412(1) |
| A2.52 | 5 | 510(10) | 21.3(3) | 1590(30) | 2510(50) | 2.625(1) |
| A2.41 | 6 | 520(10) | 22.8(3) | 1550(30) | 2360(50) | 2.572(1) |
| A2.34 | 7 | 490(10) | 23.3(3) | 1480(30) | 2240(40) | 1.868(1) |
| A2.37 | 8 | 500(10) | 24.1(3) | 1450(30) | 2160(40) | 2.013(1) |
| A2.36 | 9 | 490(10) | 24.5(3) | 1390(30) | 2080(40) | 2.427(1) |
| A2.64 | 10 | 530(10) | 27.4(3) | 1230(20) | 1770(30) | — |
| A2.57 | 11 | 2020(10) | 17.9(3) | 2310(50) | 4300(90) | 0.1495(1) |
| A2.43 | 12 | 2010(10) | 18.7(3) | 1640(30) | 2530(50) | 3.933(2) |
| A2.44 | 13 | 1990(10) | 19.2(3) | 1590(30) | 2440(50) | 4.804(2) |
| A2.48 | 14 | 2000(10) | 20.6(3) | 1590(30) | 2420(50) | 4.029(2) |
| A2.46 | 15 | 2000(10) | 21.4(3) | 1580(30) | 2380(50) | 3.858(2) |
| A2.45 | 16 | 2000(10) | 22.3(3) | 1560(30) | 2370(50) | — |
| A2.50 | 17 | 2010(10) | 23.8(3) | 1510(30) | 2280(50) | 3.529(2) |
| A2.53 | 18 | 2060(10) | 24.6(3) | 1460(30) | 2180(40) | 3.742(2) |
| A2.61 | 19 | 1990(10) | 26.8(3) | 1340(30) | 1890(40) | 0.1291(1) |
| A2.63 | 20 | 2010(10) | 27.4(3) | 1130(20) | 1580(30) | — |

of the magnetoresistance of the 500 Å and 2000 Å samples selected for magnetoresistance measurements, which have a definite minimum. By plotting these data on suitable axes, a small region of $\Delta\rho/\rho^2 \propto B^2$ dependence at low fields, and a clear $\Delta\rho/\rho^2 \propto B^{3/2}$ dependence at higher fields, may be identified. As the temperature is decreased below $T(\rho = \text{min})$, the magnitude of the positive magnetoresistance continues to increase, and reaches a maximum at some sample-dependent temperature. This sample-dependent temperature is always lower than the temperature at which the minimum in ρ occurs. As the temperature is decreased further, the magnetoresistance decreases in magnitude and eventually changes sign to become negative at low enough temperatures (shown for example for sample 2 (500 Å, 20.0 at.% Fe) in figure 2(b)). This magnetoresistance behaviour is the same as that reported previously for $\text{Fe}_x\text{Ge}_{1-x}$ samples of similar composition. The effect of the positive magnetoresistance on the anomalous decrease in ρ can be clearly seen in figure 3, where the ρ in magnetic fields between 0 and 8.5 T of samples 4 (500 Å, 20.9 at.% Fe) and 15 (2000 Å, 21.4 at.% Fe) is plotted as a function of temperature. Note that with increasing magnetic field the magnitude of the decrease in ρ , given by $\Delta\rho/\rho_{\text{min}}$, gets smaller, and the temperature at which the minimum in ρ occurs increases.

Based on their magnetization and Mössbauer effect spectroscopy measurements, previous workers (Massenet and Daver 1977, 1978, Massenet *et al* 1979) have concluded that below about 40 at.% Fe the Fe atoms in amorphous $\text{Fe}_x\text{Ge}_{1-x}$ alloys have no magnetic moment. In the present samples, magnetization measurements performed from 300 K to 6 K on five samples, with between 27 at.% Fe and 17 at.% Fe, using a SQUID magnetometer (Dumpich and Luebeck 1992), show that no magnetic ordering occurs in these samples down to 6 K. This result is consistent with the previous work referenced above.

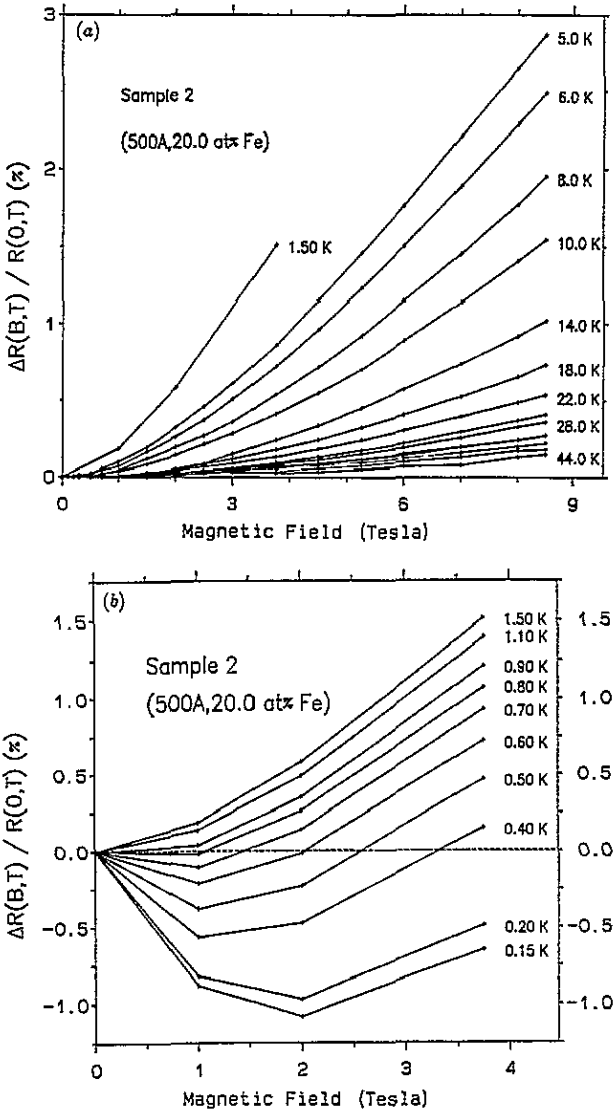


Figure 2. The magnetoresistance $\Delta R/R$ as a function of magnetic field B for sample 2 (500 Å, 20.0 at.% Fe): (a) at $1.5 \text{ K} \leq T \leq 100 \text{ K}$ in magnetic fields $B \leq 8.5 \text{ T}$; (b) at $T \leq 1.5 \text{ K}$ in magnetic fields $B \leq 3.8 \text{ T}$. The range of the magnetic field in the two sets of data is different because the data were obtained from two different experimental facilities.

4. Analysis

4.1. $T(\rho = \min) \leq T \leq T(\rho = \max)$

The ρ of amorphous metallic samples at low temperatures has usually been interpreted in terms of the theories of impurity-enhanced electron-electron interactions (Altshuler and Aronov 1979, Altshuler *et al* 1980, Fukuyama 1980, 1981) and weak localization (Gorkov *et al* 1979, Bergmann 1983a, b, 1984, Kawabata 1980a, b). The change in the conductivity due to electron-electron interaction effects in 3D films has been expressed by Lee and

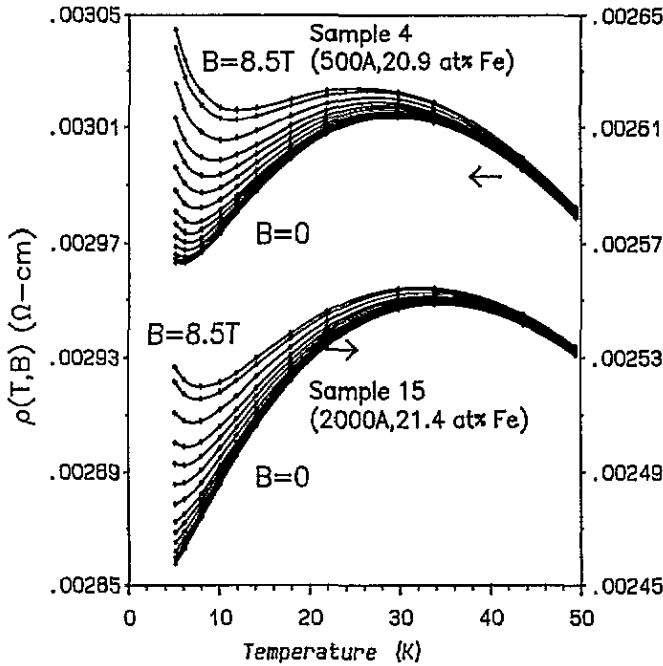


Figure 3. The measured ρ in magnetic fields $0 \leq B \leq 8.5$ T of samples 4 (500 Å, 20.9 at% Fe) and 15 (2000 Å, 21.4 at% Fe) as a function of T . In this figure the effect of the positive magnetoresistance on the decrease in ρ can be clearly seen.

Ramakrishnan (1985) in the form

$$\Delta\sigma_{EE}(T) = -\Delta\rho/\rho^2 = (e^2/4\pi^2\hbar) \left(1.3/\sqrt{2}\right) \left[\frac{4}{3} - \frac{3}{2}\tilde{F}_\sigma\right] \sqrt{T/D} \quad (1)$$

where \tilde{F}_σ is the screening parameter for the Coulomb interaction and D is the diffusion constant.

In three dimensions, the change in the conductivity due to weak localization with no spin-orbit scattering can be expressed as (Lee and Ramakrishnan 1985)

$$\Delta\sigma_{WL}(T) = -\Delta\rho/\rho^2 = + [(e^2/\hbar\pi^3)/a] T^{p/2} \quad (2)$$

where a is a microscopic-scale length of order k_F^{-1} which relates the inelastic scattering length ℓ_{in} and the temperature ($\ell_{in} = aT^{-p/2}$, so $a/1 \text{ K}^{p/2} = \ell_{in}(1 \text{ K})$), and p is an index that depends on the scattering mechanism. This weak-localization contribution to the conductivity changes sign to become negative in the presence of strong spin-orbit scattering. The temperature dependence of $\Delta\sigma_{WL}(T)$ depends on the dominant inelastic scattering mechanism through the index p : $p = 1$ for scattering by phonons (or magnons) at $T > T_D$ (or T_N); $p = 2$ for inelastic electron-electron scattering; $p = 4$ for scattering by phonons or magnons at $T < T_D$ or T_N .

As both $\Delta\sigma_{EE}(T)$ and $\Delta\sigma_{WL}(T)$ have the same form, the data fitting can be carried out using the expressions

$$\sigma(T) = \sigma_0^{EE} + G^{EE}T^x \quad (3a)$$

and

$$\sigma(T) = \sigma_0^{WL} + G^{WL}T^x \quad (3b)$$

with the appropriate value of the exponent x , and then the fitting parameters G^{EE} and G^{WL} can be interpreted using the relevant theory.

As the observed decrease in ρ below about 30 K is also very similar to the behaviour of ρ due to the influence of localized spin fluctuations (see for example Strom-Olsen *et al* 1985), it is also necessary to try to fit the measured ρ data in this temperature regime using spin fluctuation theory. According to this theory, ρ of so-called exchange-enhanced materials has the form (Rivier and Zlatic 1972)

$$\rho = A\tilde{\rho}_c = A \left\{ 1 - \left[1 + (\pi T/T_{SF}) + \psi \left(\frac{1}{2} + T_{SF}/2\pi T \right) - \psi \left(1 + T_{SF}/2\pi T \right) \right]^{-1} \right\} \quad (4)$$

where $\psi(z)$ is the digamma function, $T_{SF} = \hbar/k_B\tau_{SF}$, and τ_{SF} is the characteristic spin fluctuation lifetime. The value of $\tilde{\rho}_c$ predicted by the theory lies between zero and unity, and so it must be scaled by $A = \rho(\max) - \rho(\min)$ to fit the 'mean magnitude' of the experimental data, while T_{SF} is varied to fit the observed shape of the data.

Table 2. Values of the fit parameters obtained by fitting the ρ - T data over the indicated temperature range in the temperature regime between the maximum and the minimum in ρ using equations (3a) and (4).

| Sample | at.% Fe | Equation (3a) | | | Equation (4) | |
|--------|---------|--------------------------------------|--------------------------------------|---------------|------------------------------------|---------------|
| | | G ($\Omega^{-1} m^{-1} K^{1/2}$) | σ_0 ($\Omega^{-1} cm^{-1}$) | T range (K) | τ_{SF} ($\times 10^{-13}$ s) | T range (K) |
| 2 | 20.0(3) | $-5.25(3) \times 10^{-4}$ | 312(6) | 20.2-7.64 | 3.32(5) | 26.1-5.46 |
| 3 | 20.5(3) | $-7.83(5) \times 10^{-4}$ | 376(7) | 21.4-7.68 | 3.35(6) | 28.0-4.97 |
| 4 | 20.9(3) | $-9.89(6) \times 10^{-4}$ | 399(8) | 21.8-6.16 | 3.62(7) | 32.5-4.44 |
| 5 | 21.3(3) | $-11.22(7) \times 10^{-4}$ | 408(8) | 20.9-7.08 | — | — |
| 6 | 22.8(3) | $-10.77(7) \times 10^{-4}$ | 432(9) | 21.5-6.04 | 3.76(7) | 31.6-4.29 |
| 7 | 23.3(3) | $-9.35(6) \times 10^{-4}$ | 456(9) | 21.9-8.83 | 3.01(5) | 34.4-5.98 |
| 8 | 24.1(3) | $-9.97(6) \times 10^{-4}$ | 471(9) | 20.3-7.76 | 3.08(5) | 31.1-4.89 |
| 9 | 24.5(3) | $-12.18(8) \times 10^{-4}$ | 493(9) | 23.5-7.56 | 2.99(5) | 36.6-4.60 |
| 12 | 18.7(3) | $-14.56(1) \times 10^{-4}$ | 407(8) | 20.2-4.40 | 3.26(5) | 31.3-2.52 |
| 13 | 19.2(3) | $-17.01(1) \times 10^{-4}$ | 422(8) | 17.7-5.18 | 4.01(7) | 32.5-1.94 |
| 14 | 20.6(3) | $-15.34(1) \times 10^{-4}$ | 427(9) | 20.3-6.72 | 3.27(5) | 33.7-2.88 |
| 15 | 21.4(3) | $-15.12(1) \times 10^{-4}$ | 432(9) | 20.7-5.48 | 3.17(3) | 33.7-2.50 |
| 16 | 22.3(3) | $-15.64(1) \times 10^{-4}$ | 436(9) | 19.1-4.12 | — | — |
| 17 | 23.8(3) | $-14.43(1) \times 10^{-4}$ | 450(9) | 21.1-8.79 | 3.35(5) | 33.4-3.84 |
| 18 | 24.6(3) | $-16.15(1) \times 10^{-4}$ | 471(9) | 20.5-6.77 | 3.07(2) | 33.7-3.40 |

Between the maximum and the minimum in ρ , the positive-TCR experimental data have been fitted over limited temperature ranges using equations (3a) and (4). In (3a) the exponent was initially constrained to the value $x = 0.5$, but was later allowed to vary with virtually no resulting change in x and no improvement to the fits. The parameters obtained from the fits using the two equations are given in table 2, together with the temperature range over which the data could be fitted. The fits obtained using (3a) and (4) are shown in figures 4(a) and 4(b) respectively. Using the minimization criterion $\chi^2 = \sum [\rho_i - f(T_i)]^2 / \delta\rho_i^2$, where ρ_i and T_i constitute the i th data point, and $\delta\rho_i$ is the experimental uncertainty in ρ_i , similar values of χ^2 are obtained for the fits using (3a) and (4). It should however be noted that the fits using (3a) apply over a smaller range of T , as this equation cannot account for the flattening out of ρ close to the maximum and the minimum. The variation of the fit parameters σ_0^{EE} and G^{EE} with Fe concentration is complicated by the change in $\Delta\rho/\rho_{\min}$ and the slight differences in the gradient of the ρ - T data. It is therefore not possible to interpret the parameters σ_0^{EE} and G^{EE} obtained from the fits using (3a) in any quantitative manner.

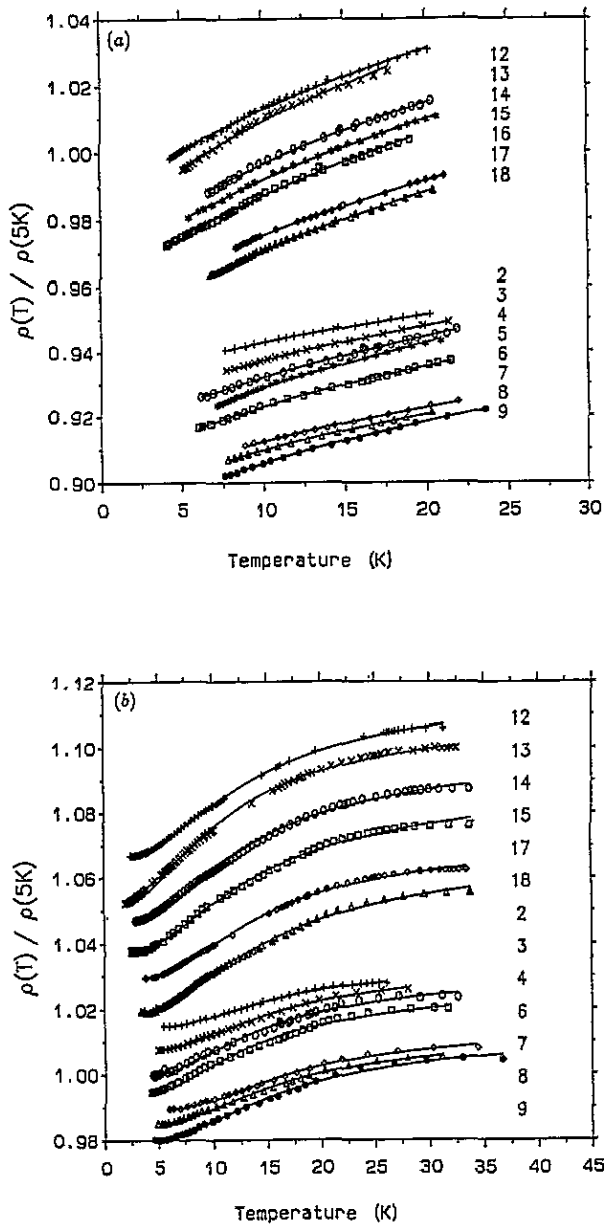


Figure 4. The fits of ρ over the temperature ranges given in table 2 in the temperature regime between the maximum and the minimum in ρ using (a) equation (3a) for the theory of impurity-enhanced electron-electron interactions; and (b) equation (4) for the theory of electron scattering from localized spin fluctuations. Note that in (b) the calculated curves extend to the lowest T of the data, but are usually lost in the experimental data. In both (a) and (b) the curves are numbered sequentially starting from the top curve, and have been displaced vertically, by somewhat arbitrary amounts, for clarity.

It may be noted however that σ_0^{EE} generally decreases with decreasing Fe concentration as expected.

The model of the resistivity due to electron scattering from localized spin fluctuations (equation (4)) has only one physical parameter, namely T_{SF} . The magnitude of ρ is determined by the scaling parameter A , which will clearly be sensitive to the variation in $\Delta\rho/\rho_{\text{min}}$ and to the gradient of the ρ - T data, as were the fitting parameters in (3a). However, the parameter T_{SF} , which parameterizes the range of the temperature between the minimum and the maximum in ρ , should not be influenced by these variations as it determines only the normalized temperature variation. From table 2 it is observed that τ_{SF} is essentially independent of the Fe concentration, as is expected (see for example Rossiter 1987).

Analytical expressions for the magnetoconductivity due to weak localization and impurity-enhanced electron-electron interactions are available in the literature in forms which are useful for fitting purposes (see for example Baxter *et al* 1989). However, attempts to fit the magnetoresistance data of the present samples (as shown for example in figure 2(a)) using either the 2D or 3D expressions from these theories were not successful. For all the samples, the magnetoresistance calculated using the theories could not reproduce the observed B dependence of the measured data, and the magnitude of the calculated magnetoresistance was significantly smaller than the magnitude of the measured effect. Magnetoresistance data with similar shape and magnitude have been reported in the literature for the amorphous paramagnetic Zr-Fe system, where the observations were attributed to the effects of spin fluctuations (Trudeau and Cochrane 1988). As no explicit expression for the magnetoconductivity due to spin fluctuations at finite temperatures has thus far been published, those authors utilized an enhanced Zeeman splitting of the spin subbands to include the effects of spin fluctuations to the theories of the magnetoconductivity due to weak localization and impurity-enhanced electron-electron interactions. The magnetoresistance of the present amorphous $\text{Fe}_x\text{Ge}_{1-x}$ samples could not be fitted satisfactorily using this technique. The magnitude of the magnetoresistance calculated using this technique for either weak localization or electron-electron interactions, or a combination of both contributions, was closer to but still significantly smaller than the observed magnitude. Although the magnetoresistance could be reasonably fitted at any one temperature using a very much enhanced Zeeman splitting, the full set of data at all the fixed temperatures could not be fitted in a self-consistent manner using the predicted B and T dependences of the theories.

As the existing models which are believed to be relevant in amorphous alloys are not able to fit the measured magnetoresistance, the data have been fitted using phenomenological expressions. The magnetoconductivity at each temperature may be divided into a high-field regime and a low-field regime, separated by a sample- (i.e. composition-) and temperature-dependent magnetic field $B_{\infty}(T, \text{sample})$.

In the low-field regime, the data have been fitted using the expression

$$\frac{\Delta\rho}{\rho^2} = A + CB^2 \quad (5)$$

with fitting parameters of the intercept A and the coefficient of the quadratic term C . In the high-field regime, the data have been fitted using the expression

$$\frac{\Delta\rho}{\rho^2} = P + QB^{3/2} \quad (6)$$

with fitting parameters of the intercept P and the coefficient of the $B^{3/2}$ term Q . An example of the phenomenological theoretical curves obtained using these expressions is shown in figure 5 for sample 2 (500 Å, 20.0 at.% Fe). The values of the parameters C , P , and Q , together with the values of $B_{\infty}(T, \text{sample})$, are given in table 3, at three representative temperatures for the five 500 Å samples and the five 2000 Å samples selected

Table 3. Values of the fit parameters at three representative temperatures obtained by fitting the magnetoresistance data of the samples in the low- and high-field regimes using equations (5) and (6) respectively. The parameter B_{co} (T) indicates the maximum or minimum magnetic field data included in the fit using equation (5) or (6). For all the samples measured, within the uncertainty of the data, the parameter A in equation (5) is zero.

| Sample | at.% Fe | Equation (5) | | | Equation (6) | | | |
|--------|---------|--------------|--------------|---|--------------|--------------|---------------------------------------|--|
| | | T (K) | B_{co} (T) | C ($\Omega^{-1} \text{ cm}^{-1} \text{ T}^{1/2}$) | T (K) | B_{co} (T) | P ($\Omega^{-1} \text{ cm}^{-1}$) | Q ($\Omega^{-1} \text{ cm}^{-1} \text{ T}^{-3/2}$) |
| 1 | 18.8(3) | 5.0 | 1.5 | 0.18(1) | 5.0 | 2.0 | -0.0117(1) | 0.235(1) |
| | | 18.0 | 3.0 | 0.027(3) | 29.5 | 3.75 | -0.0794(1) | 0.0296(1) |
| | | 29.5 | 3.75 | 0.010(1) | 49.8 | 3.75 | -0.0416(1) | 0.0183(1) |
| 2 | 20.0(3) | 5.0 | 1.0 | 0.30(5) | 5.0 | 2.0 | -0.0503(2) | 0.358(1) |
| | | 17.8 | 3.0 | 0.041(6) | 29.9 | 3.75 | -0.0673(1) | 0.0401(1) |
| | | 29.9 | 3.75 | 0.015(2) | 49.7 | 3.75 | -0.0569(1) | 0.0178(1) |
| 4 | 20.9(3) | 5.1 | 2.0 | 0.26(1) | 5.1 | 2.0 | -0.0410(2) | 0.387(1) |
| | | 18.0 | 3.0 | 0.040(6) | 29.8 | 3.75 | -0.0931(2) | 0.0442(1) |
| | | 29.8 | 3.75 | 0.017(3) | 49.6 | 4.5 | -0.0832(1) | 0.0192(1) |
| 9 | 24.5(3) | 4.9 | 1.0 | 0.38(9) | 5.0 | 1.0 | -0.115(1) | 0.507(1) |
| | | 17.8 | 3.0 | 0.056(9) | 30.0 | 3.75 | -0.0860(1) | 0.0588(1) |
| | | 30.0 | 3.75 | 0.023(4) | 49.7 | 3.75 | -0.114(1) | 0.0297(1) |
| 10 | 27.4(3) | — | — | — | 5.0 | 4.5 | -0.251(1) | 0.0235(1) |
| | | — | — | — | 29.5 | 2.5 | -0.0441(1) | 0.0207(1) |
| | | — | — | — | 49.4 | 1.5 | -0.0285(1) | 0.0103(1) |
| 11 | 17.9(3) | 5.0 | 0.7 | 0.31(9) | 5.0 | 0.7 | -0.0596(1) | 0.359(1) |
| | | 18.0 | 3.75 | 0.033(3) | 29.7 | 3.0 | -0.0721(1) | 0.0823(1) |
| | | 29.7 | 3.0 | 0.011(4) | 49.8 | 3.0 | -0.0339(1) | 0.0183(1) |
| 12 | 18.7(3) | — | — | — | 5.1 | 0.7 | -0.0899(1) | 0.450(1) |
| | | — | — | — | 29.5 | 1.5 | -0.0536(1) | 0.0416(1) |
| | | — | — | — | 49.8 | 3.75 | -0.0793(1) | 0.0197(1) |
| 15 | 21.4(3) | 5.1 | 1.0 | 0.37(7) | 5.1 | 1.0 | -0.113(1) | 0.482(1) |
| | | 18.0 | 3.75 | 0.044(4) | 29.9 | 3.75 | -0.124(1) | 0.0491(1) |
| | | 29.9 | 3.75 | 0.020(3) | 49.6 | 3.75 | -0.0757(1) | 0.0191(1) |
| 18 | 24.6(3) | 5.1 | 0.7 | 0.40(18) | 5.1 | 0.7 | -0.0929(2) | 0.503(1) |
| | | 21.7 | 3.0 | 0.035(8) | 29.7 | 2.5 | -0.0746(1) | 0.0503(1) |
| | | 29.7 | 2.5 | 0.017(13) | 49.8 | 5.25 | -0.135(1) | 0.0265(1) |
| 20 | 27.4(3) | 12.0 | 1.0 | 0.13(13) | 5.0 | 5.25 | -1.165(1) | 0.0989(1) |
| | | 14.0 | 1.5 | 0.11(6) | 29.5 | 3.75 | -0.181(1) | 0.101(1) |
| | | 17.9 | 1.5 | 0.09(6) | 49.5 | 3.75 | -0.126(1) | 0.0507(1) |

for magnetoresistance measurements. For all these samples, within the uncertainty of the data, the intercept A in the low-field fits is zero. This is to be expected if the $\Delta\rho/\rho^2 \propto B^2$ dependence exists down to zero field. The values of the parameters C and Q obtained from the fits of the magnetoconductance are plotted against $1/T$ in figure 6. From this figure it can be seen that for the 500 Å samples with between about 25 at.% Fe and about 18 at.% Fe, C is proportional to $1/T$ between about 5 K and 20 K, with some deviations from this dependence evident above 20 K. Above about 25 at.% Fe the relatively large statistical uncertainties on the values of C make it impossible to discern any particular temperature dependence. As can be seen from figure 6, a similar $1/T$ dependence is evident in the parameter Q in the 500 Å samples with between about 25 at.% Fe and about 18 at.% Fe. This dependence is evident at all temperatures between about 8 K and 50 K in the 500 Å samples, with deviations to a weaker temperature dependence below about 8 K. The

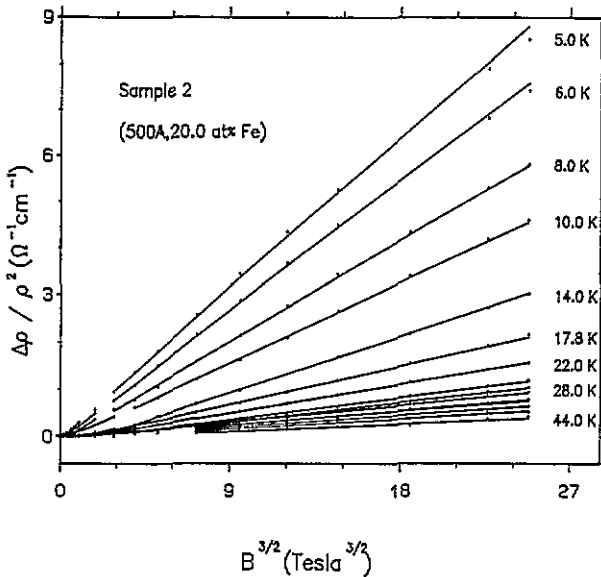


Figure 5. The fits of the magnetoconductivity $\Delta\rho/\rho^2$ of sample 2 (500 Å, 20.0 at% Fe) at temperatures $5\text{ K} \leq T \leq 44\text{ K}$ in magnetic fields $B \leq 8.5\text{ T}$ using the phenomenological expressions (5) and (6). These fits are typical of the fits obtained for all the samples selected for magnetoresistance measurements.

parameters C and Q obtained from the fits of the magnetoresistance of the 2000 Å samples show a similar $1/T$ dependence, although the $Q \propto 1/T$ dependence is in this case evident down to 5 K. The values of the parameter Q for the 500 Å and 2000 Å samples with 27.4 at% Fe are clearly observable, but do not show any clear temperature dependence. Both of the parameters C and Q have a maximum in their magnitude close to 24.5 at% Fe.

4.2. $T < T(\rho = \min)$

The increase in ρ as the temperature decreases below about 4 K has previously been tentatively interpreted as due to weak localization (Mott 1990, Mott and Davis 1991, Albers and McLachlan 1993). This interpretation has been based on two observations: the $\rho \propto \sqrt{T}$ dependence and the negative magnetoresistance, both observed at low enough temperatures in previous measurements (Albers and McLachlan 1993) and in the present samples. Although a $\rho \propto \sqrt{T}$ dependence is also expected due to impurity-enhanced electron-electron interactions (see equation (1)), the magnetoresistance due to this mechanism is positive, which is contrary to the observed negative magnetoresistance at low enough temperatures in the present samples. The measured ρ data in this temperature regime have thus been fitted using (3b) over limited temperature ranges. The exponent in (3b) was initially constrained to $x = 0.5$, but did not show any significant deviation from that value when it was later allowed to vary. The parameters obtained from the fits and the temperature ranges over which the fitting was carried out are given in table 4. The theoretical curves together with the experimental data are shown in figure 7, where the resistivity of each sample has been normalized to the value of $\rho(0.9\text{ K})$ (500 Å samples) or $\rho(0.5\text{ K})$ (2000 Å samples) (the highest temperature included in the fits of all the samples). The values of ρ used for the normalization are given in the column labelled $\rho(\text{Norm})$ in table 4. Note that

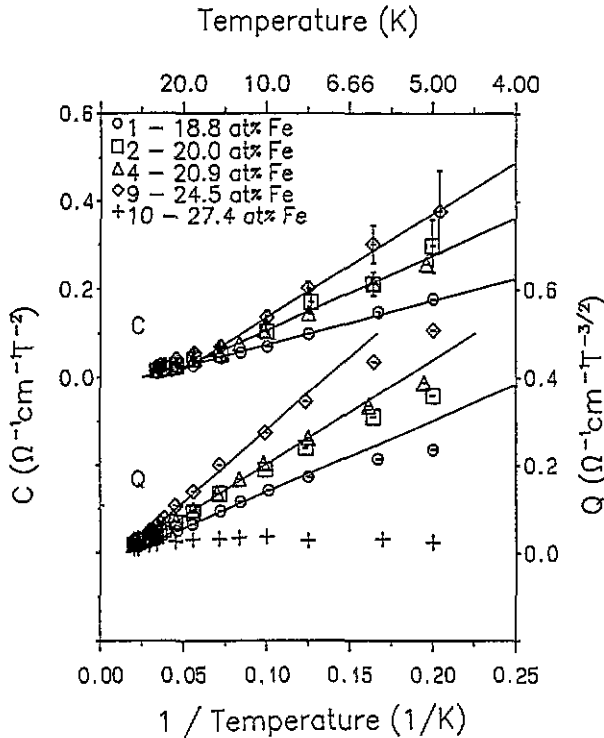


Figure 6. The values of the fit parameters C and Q in (5) and (6) as functions of $1/T$ for all the nominally 500 Å and 2000 Å samples selected for magnetoresistance measurements.

sample 10 (500 Å) and sample 20 (2000 Å), both with 27.4 at.% Fe could be fitted using (3b) to significantly higher temperatures than the other samples. This is almost certainly due to the fact that both of these samples only show an inflection as T decreases below 30 K, and so the $\rho \propto \sqrt{T}$ dependence is evident at higher temperatures.

Table 4. Values of the fit parameters obtained by fitting the ρ - T data over the indicated temperature range in the temperature regime below the minimum in ρ using equation (3b). The values of $\rho(\text{Norm})$ (where Norm = 0.5 K and Norm = 0.9 K for the nominally 500 Å and 2000 Å samples respectively) are used to normalize the ρ - T data and the fits shown in figure (8).

| Sample | at.% Fe | Equation (3b) | | | |
|--------|---------|---|--|--|---------------|
| | | G ($10^3 \Omega^{-1} \text{ m}^{-1} \text{ K}^{1/2}$) | σ_0 ($\Omega^{-1} \text{ cm}^{-1}$) | $\rho(\text{Norm})$ ($\mu\Omega \text{ cm}$) | T range (K) |
| 1 | 18.8(3) | 3.321(6) | 109(2) | 7095 | 0.90–0.25 |
| 2 | 20.0(3) | 2.42(1) | 255(5) | 3604 | 0.90–0.082 |
| 9 | 24.5(3) | 2.88(1) | 477(9) | 1979 | 1.103–0.082 |
| 10 | 27.4(3) | 2.552(5) | 510(10) | 1880 | 5.096–0.25 |
| 11 | 17.9(3) | 4.79(3) | 163(3) | 5078 | 0.50–0.297 |
| 15 | 21.4(3) | 2.33(2) | 385(8) | 2488 | 0.80–0.15 |
| 18 | 24.6(3) | 2.46(4) | 413(8) | 2319 | 0.90–0.40 |
| 20 | 27.4(3) | 2.56(1) | 565(11) | 1714 | 5.10–0.25 |

The values of the fitting parameters σ_0^{WL} and G^{WL} are plotted against Fe concentration

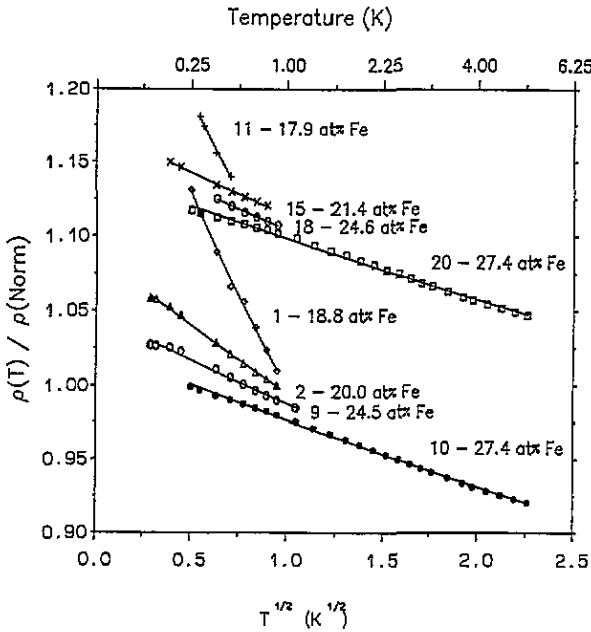


Figure 7. The fits of ρ over limited ranges of T in the T regime below the minimum in ρ using (3b) for the theory of weak localization. Note that samples 10 (500 Å) and 20 (2000 Å), both with 27.4 at.% Fe, do not show the decrease in ρ as T decreases below about 30 K, observed in the other samples shown in the figure, and hence the $\rho \propto \sqrt{T}$ dependence is observed at higher temperatures.

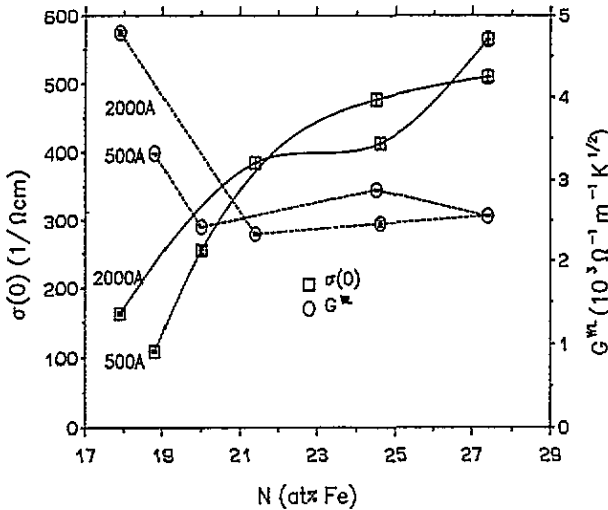


Figure 8. The values of the fit parameters σ_0^{WL} and G^{WL} obtained from the fits of ρ in the temperature regime below the minimum in ρ using equation (3b).

in figure 8. The parameter σ_0^{WL} behaves in a manner which is consistent with expectations, showing $\sigma_0^{WL} \rightarrow 0$ with decreasing Fe concentration as the metal-insulator transition at about 16 at.% Fe (Albers and McLachlan 1993) is approached. The parameter $G^{WL} =$

$(e^2/\hbar\pi^3)(1/a)$ (from (2) and (3b)) remains essentially constant between 27.4 at.% Fe and about 20 at.% Fe, but then increases when the Fe concentration is decreased further. This increase in G^{WL} below about 20 at.% Fe corresponds to a decrease in the value of a , i.e. a decrease in the inelastic scattering length $\ell_{\text{in}}(1\text{K})$.

The magnetoresistance in the temperature regime below the minimum in ρ , shown for example for sample 2 (500 Å, 20.0 at.% Fe) in figure 2(b), shows the changeover from the positive magnetoresistance observed at $T(\rho = \min) \leq T \leq T(\rho = \max)$, discussed above, to the negative magnetoresistance observed at low enough temperatures in all the measured samples. Because of the sign, the negative magnetoresistance observed in low B is at least *qualitatively* consistent with the theory of weak-localization. Although no clear field dependence can be distinguished in the data, the $\Delta\rho/\rho^2 \propto \sqrt{B}$ dependence at higher B predicted by weak-localization theory is clearly not observed in the data. Instead, the magnitude of the magnetoresistance reaches a maximum at about 2.5 T and then decreases, with the sign of the magnetoresistance changing to positive at high enough B at temperatures which are not too low (see the $T = 0.4$ K curve in figure 2(b)). This decrease in the magnitude of the magnetoresistance in $B \geq 2.5$ T at the lowest temperatures may be due to the influence of the mechanism responsible for the positive magnetoresistance at higher temperatures taking over the dominance from the (virtually saturated) negative $\Delta\rho/\rho^2 \propto \sqrt{B}$ dependence.

5. Discussion

Comparing the ρ against T and magnetoresistance data of the 500 Å and the 2000 Å samples below about 30 K, the following three primary differences are evident. First, the magnitude of the decrease in ρ , given by $\Delta\rho/\rho_{\text{min}}$ in table 1, is consistently larger in the 2000 Å samples. This is reflected in the observation that the gradient of the ρ against T data in the temperature regime between $T(\rho = \min)$ and $T(\rho = \max)$, given by the parameter G^{EE} in table 2, is consistently larger in magnitude for the 2000 Å samples. Second, the minimum in ρ occurs consistently about 2 K lower in the 2000 Å samples than in the 500 Å samples. Third, it is evident that the magnitude of both the positive magnetoresistance observed at higher T and the negative magnetoresistance observed at lower T is consistently larger in the 2000 Å samples than in the 500 Å samples. These differences between the 500 Å samples and the 2000 Å samples appear to indicate that the effect of the mechanism responsible for the decrease in ρ with decreasing T is stronger in the thicker samples. If the origin of the decrease in ρ is magnetic, it could be speculated that surface proximity effects may play a role in reducing the total number of magnetic scattering centres, thus reducing the magnitude of the magnetic scattering contribution to ρ . Such surface proximity effects would clearly have a larger relative effect in the thinner samples. An alternative speculation is that although the characteristic lengths of the system are estimated to be about 100 Å, the characteristic length of one of the conduction mechanisms may be close to 500 Å, with a resulting modification to that contribution to the resistivity. Although the above-mentioned differences between the 500 Å and 2000 Å samples are significant, the results are qualitatively the same and do not indicate that the 500 Å samples are not 3D.

The ρ data in the two temperature regimes ($T(\rho = \min) \leq T \leq T(\rho = \max)$ and $T < T(\rho = \min)$) can be fitted reasonably well using (3). However, although the parameter σ_0 in each of the temperature regimes behaves as expected, the parameter G does not appear to show any consistent behaviour. The fits of ρ between the minimum and the maximum in ρ using the theory of electron scattering from localized spin fluctuations using (4) are qualitatively as good as the fits using (3a), and the value of τ_{SF} obtained from the fits is

essentially independent of the Fe concentration as expected (see for example Rossiter 1987).

The magnetoresistance at temperatures between the minimum and the maximum in ρ is not consistent with the available theories of impurity-enhanced electron–electron interactions and weak localization, and cannot either be fitted using the method successfully used by Trudeau and Cochrane (1988) to account for the effects of spin fluctuations on these two theories. The magnetoresistance in this temperature regime, which is almost certainly due to the mechanism responsible for the observed decrease in ρ with decreasing T , has the following characteristic field and temperature dependences: $\Delta\rho/\rho^2 \propto B^2$ at low B , with a $1/T$ dependence in the proportionality constant between about 5 K and 20 K; and $\Delta\rho/\rho^2 \propto B^{3/2}$ at high B , also with a $1/T$ dependence in the proportionality constant but in this case between about 8 K and 50 K. As expected, in the temperature region from 5 K to 6 K (where the measurements overlap), no difference is observed between the magnetoresistance measured with $B \perp$ the plane of the sample and that measured with $B \parallel$ the plane of the sample. The negative magnetoresistance observed at low enough temperatures below $T(\rho = \min)$ is at least qualitatively consistent with the theory of weak localization, indicating that the \sqrt{T} dependence observed in ρ at the lowest temperatures is probably due to weak localization.

Although the specific conduction mechanism responsible for the observed decrease in ρ with decreasing T below about 30 K has not been unambiguously identified, the disagreement in the magnitude, the B dependence and the T dependence between the measured magnetoresistance and the existing theories of weak localization and impurity-enhanced electron–electron interactions appears to indicate that neither of these two mechanisms are responsible. The field dependences observed in the magnetoresistance therefore provide constraints which possible models of the conduction mechanisms must satisfy. As the decrease in ρ in amorphous alloys of Ge or Si has only been observed in alloys containing magnetic atoms (Fe or Cr), it seems probable that the decrease in ρ is associated with the magnetism of the alloy, even though there is apparently no magnetic moment on the Fe atoms in these amorphous metallic Fe_xGe_{1-x} alloys. It would therefore be of interest to investigate amorphous alloys of Ge or Si with other magnetic elements to determine whether this phenomenon is observed in those alloys as well, to try to identify any relationship between the decrease in ρ and the magnitude of the magnetic moment of the ion of the particular element.

References

- Albers A 1994 *PhD Thesis* University of the Witwatersrand
 Albers A and McLachlan D S 1993 *J. Phys.: Condens. Matter* **5** 6067
 Altshuler B L and Aronov A G 1979 *Solid State Commun.* **30** 115
 Altshuler B L, Aronov A G and Lee P A 1980 *Phys. Rev. Lett.* **44** 1288
 Baxter D V, Richter R, Trudeau M L, Cochrane R W and Strom-Olsen J O 1989 *J. Physique* **50** 1673
 Bergmann G 1983a *Phys. Rev. B* **28** 515
 —1983b *Phys. Rev. B* **28** 2914
 —1984 *Phys. Rep.* **107** 1
 Dumpich G and Luebeck Th 1992 private communication
 Elefant D, Gladun C, Heinrich A, Schumann J and Vinzelberg H 1991 *Phil. Mag.* **B 64** 49
 Fukuyama H 1980 *J. Phys. Soc. Japan* **48** 2169
 —1981 *J. Phys. Soc. Japan* **50** 3407
 Gorkov L P, Larkin A I and Khmel'nitskii D E 1979 *JETP Lett.* **30** 228
 Kawabata A 1980a *Solid State Commun.* **34** 431
 —1980b *J. Phys. Soc. Japan* **49** 628
 Lee P A and Ramakrishnan T V 1985 *Rev. Mod. Phys.* **57** 287

- Massenet O and Daver H 1977 *Solid State Commun.* **21** 37
—1978 *Solid State Commun.* **25** 917
- Massenet O, Daver H, Nguyen V D and Rebouillat J P 1979 *J. Phys. F: Met. Phys.* **9** 1687
- Möbius A, Vinzelberg H, Gladun C, Heinrich A, Elefant D, Schumann J and Ziess G 1985 *J. Phys. C: Solid State Phys.* **18** 3337
- Mooij J H 1973 *Phys. Status Solidi a* **17** 521
- Mott N F 1990 *Localization 1990: Proc. Int. Conf. on Localization (Inst. Phys. Conf. Ser. 108)* ed K A Benedict and J T Chalker (Bristol: Institute of Physics) p 1
- Mott N F and Davis E A 1991 private communication
- Rivier N and Zlatic V 1972 *J. Phys. F: Met. Phys.* **2** L99
- Rossiter P L 1987 *The Electrical Resistivity of Metals and Alloys* (Cambridge: Cambridge University Press)
- Strom-Olsen J O, Altounian Z, Cochrane R W and Kaiser A B 1985 *Phys. Rev. B* **31** 6116
- Trudeau M L and Cochrane R W 1988 *Phys. Rev. B* **38** 5353